



Published in final edited form as:

J Glaucoma. 2017 November ; 26(11): 974–979. doi:10.1097/IJG.0000000000000788.

Reproducibility and Agreement of Anterior Segment Parameter Measurements Obtained Using the CASIA2 and Spectralis OCT2 Optical Coherence Tomography Devices

Benjamin Y. Xu, MD, PhD^{#,1}, Derek D. Mai, MD¹, Rafaella C. Penteado, MD¹, Luke Saunders¹, and Robert N. Weinreb, MD¹

¹Hamilton Glaucoma Center, Shiley Eye Institute, Department of Ophthalmology, University of California, San Diego, La Jolla, CA

Abstract

Purpose—To assess the reproducibility and agreement of measurement values obtained from the Tomey CASIA2 and Heidelberg Spectralis OCT2 anterior segment optical coherence tomography (AS-OCT) devices.

Methods—Twenty eyes from ten subjects ranging from age 28 to 45 years with no history of eye conditions or intraocular surgery were included. Two scans were obtained with each device in a standardized dark-room environment after a period of dark adaptation. One AS-OCT image along the horizontal (temporal-nasal) meridian was analyzed per eye and per scan. Lens vault (LV), pupil diameter (PD), anterior chamber width (ACW), angle opening distance (AOD), trabecular iris space area (TISA), and scleral spur angle (SSAngle) were measured using manufacturer-provided image analysis programs. Intra-class correlation (ICC) values, coefficients of variation, and Bland-Altman plots were computed to assess the intra-device correlation and inter-device agreement of measurement values.

Results—There was excellent intra-device reproducibility of measurement values for both the CASIA (ICC range 0.86 to 0.99) and Spectralis (ICC range 0.79 to 1.00). There was also excellent inter-device correlation of measurement values (ICC range 0.78 to 0.93) for all parameters except ACW (ICC 0.20). Linear regression models and Bland-Altman plots showed that this relationship was strongest when measurement values were small.

[#]to whom correspondence should be addressed: Benjamin Xu, USC Gayle and Edward Roski Eye Institute, Department of Ophthalmology, Keck School of Medicine of the University of Southern California, 1450 San Pablo Street, Suite 4700, Los Angeles, CA 90033, Phone number: 323-442-6780, Fax number: 323-442-6412, benjamin.xu@med.usc.edu.

Commercial Disclosures:

1. **Benjamin Y. Xu:** none
2. **Derek D. Mai:** none
3. **Rafaella C. Penteado:** none
4. **Luke Saunders:** none
5. **Robert N. Weinreb:** C: Aerie Pharmaceutical, Alcon, Allergan, Bausch & Lomb, Eyenovia; F: Heidelberg Engineering, Carl Zeiss Meditec, Genentech, Optos, Optovue, Quark, Tomey, Topcon

Conclusion—There is excellent intra-device reproducibility and good inter-device agreement of anterior segment parameter measurement values for the CASIA2 and Spectralis OCT2. However, the measurements obtained with each device should not be considered interchangeable.

Introduction

Modern anterior segment optical coherence tomography (AS-OCT) devices are capable of producing high-resolution images of the anterior chamber and drainage angle. This has facilitated the study of a variety of topics including anatomical changes after pupillary dilation and peripheral iridotomy, post-surgical changes after cataract surgery and trabeculectomy, and risk factors for the development of gonioscopic angle closure.¹⁻⁹

Despite being a relatively new imaging modality, AS-OCT has undergone several generations of technological innovation. Time-domain (TD) OCT devices were the first to be adopted for clinical and scientific imaging of the anterior segment.¹⁰ These devices used 1310 nm wavelength light to acquire single cross-sectional images of the entire anterior chamber. Based on older OCT technology, these devices were limited in terms of imaging speed and resolution when compared to modern spectral-domain (SD) OCT devices.

SD-OCT devices have been widely adopted for posterior segment imaging, but some, including the Spectralis OCT (Heidelberg Engineering, Heidelberg, Germany), are also equipped and FDA approved for anterior segment imaging. The Spectralis uses shorter 880 nm wavelength light to produce higher axial-resolution images than TD-OCT devices, which permits visualization of intraocular structures such as Schwalbe's line and Schlemm's canal.^{11,12} However, the shorter wavelength also results in a shorter imaging range, which precludes visualization of the entire anterior chamber in a single scan.

The Tomey CASIA SS-1000 (Tomey Corporation, Nagoya, Japan) is a swept-source SD-OCT device that prioritizes rapid imaging of the entire anterior chamber over detailed imaging of a single section. The Tomey uses 1310 nm wavelength light similar to earlier TD-OCT devices, but is capable of acquiring 128 cross-sectional images in the span of a few seconds to create pseudo-three-dimensional representations of the anterior chamber. Recent studies have utilized this device to elucidate anatomical variations within the angle, providing support for its multi-image scanning approach.^{13,14}

AS-OCT devices offer an alternative to gonioscopy in qualitative assessments of the iridocorneal angle and provide a non-invasive method to quantitatively measure anterior segment parameters. In order for the utility of such measurements to become widely accepted, their repeatability must be ascertained. Furthermore, since several devices with different acquisition speeds, resolution, and laser wavelengths are commercially available, it is important to assess their level of agreement to determine if their results are interchangeable. This study seeks to address these issues by assessing the intra-device reproducibility and inter-device agreement of two next-generation devices, the Tomey CASIA2 and Heidelberg Spectralis with OCT2 Module.

Methods

Image Acquisition

Twenty eyes of ten healthy volunteers from the Shiley Eye Institute and Hamilton Glaucoma Center in San Diego, California were recruited for participation in this study. Subjects had no history or evidence of ocular disease on baseline exam, which included slit lamp and undilated fundoscopic examination. Subjects with a history of prior eye procedures, including laser peripheral iridotomy and cataract surgery, were excluded. Ethics committee approval was obtained from the University of California San Diego Medical Center Institutional Review Board. All study procedures adhered to the recommendations of the Declaration of Helsinki.

All subjects underwent non-mydriatic AS-OCT imaging of both eyes using the Tomey CASIA2 and Heidelberg Spectralis with OCT2 and Anterior Segment Modules (Figure 1). The CASIA is not FDA-approved. Two consecutive scans were performed on the CASIA in 'AC Angle' mode after 5 minutes of adaptation under dark room conditions standardized to 1 cd/m² at the imaging plane. Luminance was measured with a light meter (Light Meter 840021; Sper Scientific, Scottsdale, AZ). Two consecutive scans were then performed on the Spectralis in 'Angle' mode with EDI enabled and maximum ART of 25. For the CASIA, scans were centered over the cornea and each scan session produced 128 cross-sectional images evenly spaced 1.4 degrees apart. For the Spectralis, single image cross-sectional scans were performed along the horizontal (temporal-nasal) meridian and perpendicular to the corneal limbus.

Measurement of Parameters

Data analysis was performed on OCT images obtained from both eyes for each of the ten subjects. One trained observer (D.D.M.) masked to the identities and examination results of the subjects marked the scleral spurs and identified the angle structures in each image. The scleral spur was defined as the inward protrusion of the sclera where a change in curvature of the corneoscleral junction was observed.¹⁵ Anterior segment parameter measurements were obtained from the images using built-in software and measurement tools provided by the manufacturers. The CASIA software automatically segmented intraocular structures and generated measurement values after scleral spurs were marked. The Spectralis images required manual measurement of all parameters using the built-in Heidelberg image acquisition and viewing software. The caliper functions are non-FDA approved and were enabled by the manufacturer for research purposes under IRB approval. Six anterior segment parameters were measured in each image. Three parameters described different properties of the anterior chamber: lens vault (LV), anterior chamber width (ACW), and pupil diameter (PD). Three parameters described the drainage angle: opening distance (AOD), trabecular iris space area (TISA), and scleral spur angle (SSAngle) measured at 750 μm from the scleral spur, which approximates the width of the trabecular meshwork.^{16,17} Measurements at 250 and 500 μm from the scleral spur were not performed in order to limit the amount of manual image analysis.

Statistical Analysis

The mean and standard deviation were calculated for each set of measurement values. Intra-device and inter-device measurement correlations were calculated in the form of intra-class correlation coefficients (ICC), coefficients of variation (CoV), defined as the standard deviation of the measurement difference divided by the mean, and Bland-Altman plots with mean difference and limits of agreement (LoA). Intra-device comparisons in eyes with pupil diameters differing by more than 10 percent between the two scans were excluded from analysis to minimize the effects of pupil size on measurement values.¹⁸ Linear regression models were used to establish the relationship between inter-device measurement values. All data analysis was performed using MATLAB (Mathworks, Natick, MA).

Results

The age of the subjects ranged from 28 to 45 years (mean 37 years). There were 6 males and 4 females.

Intra-device reproducibility of measurement values for the CASIA and Spectralis

OCT images from 20 individual eyes, 10 right and 10 left, were analyzed. The scleral spur was successfully identified in all of the images. One set of measurements (one eye out of 20) was excluded from analysis in each of the intra-device comparison groups due to pupil diameters differing by more than 10 percent.

There was excellent intra-device reproducibility of measurement values for all parameters on the CASIA (Figure 2, Table 1).¹⁹ ICC values ranged from 0.86 (ACW) to 0.99 (LV). Bland-Altman plots demonstrated excellent agreement between the two sets of measurement values. The coefficients of variation ranged from 0.87% (ACW) to 14.87% (SSAngle750) for all parameters except LV (69.29%), which had a mean approaching 0 (0.07 mm).

There was also excellent intra-device reproducibility of measurement values for all parameters on the Spectralis (Figure 3, Table 2). ICC values ranged from 0.79 (ACW) to 0.99 (LV, PD). Bland-Altman plots demonstrated excellent agreement between the two sets of measurement values. The coefficients of variation ranged from 0.82% (ACW) to 10.51% (TISA750) for all parameters except LV (17.89%), which had a mean approaching 0 (0.20 mm).

Inter-device agreement of measurement values between the CASIA and Spectralis

Inter-device agreement of anterior chamber measurement values was variable (Figure 4, Table 3). For ACW, measurement values were consistently smaller for the CASIA than the Spectralis, but the correlation between the two sets of values was poor (ICC 0.20). The linear regression model of ACW had a slope of 0.82 and r^2 value of 0.35. The Bland-Altman plot demonstrated poor agreement between ACW values. Measurement values for PD and LV were consistently smaller for the CASIA than the Spectralis, although r^2 values for the linear regression models were higher (0.84 and 0.96, respectively). ICC values (0.90 and 0.93, respectively) indicated a better correlation between measurement values.

Agreement was more consistent for the angle measurement values (AOD750, TISA750, SSAngle750). For these parameters, measurement values were consistently larger for the CASIA than the Spectralis. The slopes of the linear regression models ranged from 1.24 to 1.40 and r^2 values ranged from 0.76 to 0.87. ICC values (0.78 to 0.81) indicated good correlation between the measurement values. Bland-Altman plots reflected good agreement for smaller measurement values that decreased as measurement values increased.

Discussion

This is the first study to compare anterior segment measurements from the CASIA2 device to measurements from another SD-OCT device, the Spectralis with OCT2 Module. The CASIA and Spectralis both demonstrated excellent intra-device reproducibility of measurement values for all parameters. Inter-device correlation of measurement values was variable, ranging from poor for ACW to excellent for the remainder of the parameters. In general, measurement values from the CASIA were smaller for anterior chamber parameters (PD, ACW, LV) and larger for angle parameters (AOD750, TISA750, SSAngle750) compared to the Spectralis. Also, inter-device agreement tended to worsen as measurement values increased for the angle parameters.

The CASIA and Spectralis achieved similar intra-device measurement reproducibility that is comparable to previous AS-OCT devices.^{16,20,21} However, the two devices employ different approaches to anterior segment imaging: the CASIA2 is a dedicated AS-OCT device while the Spectralis is a modular OCT device with anterior segment capabilities. As a result, there are noticeable differences in working with the devices, especially in terms of image quality and how measurements are obtained. The Spectralis produces higher axial-resolution images due to its shorter OCT wavelength and uses intra-scan image registration and averaging to improve signal-to-noise. However, due to the shorter wavelength, we had more difficulty visualizing the angle recess on Spectralis images, which is why angle recess based parameters, such as angle recess area (ARA) and trabecular iris angle (TIA), were not included in the analysis. Image averaging could also introduce artifacts in scleral spur location, although this did not greatly diminish measurement reproducibility or our ability to identify the scleral spur location. The two devices also provide different image analysis experiences. The built-in CASIA image analysis process is largely automated, requiring only that the observer confirm the structural segmentation and identify the scleral spurs. In contrast, Spectralis measurements of each parameter were obtained in a manual fashion using built-in caliper tools. Our results validate both approaches and demonstrate that automated and manual methods are equally viable for measuring anterior segment parameters, albeit the automated approach is a more time-efficient one.

While anterior segment measurements are reproducible within the CASIA and Spectralis, they differ between the two devices. Previous studies have compared measurement values between other OCT devices. One study comparing measurement values obtained from two TD-OCT devices found that their agreement was poor.²² More recent studies have found improved agreement between SD-OCT devices for both anterior and posterior segment imaging.^{20,23} Although our data show excellent agreement for the majority of parameters, this effect is primarily a result of agreement among smaller measurement values. As

measurement values increase, there appears to be a scaling effect that causes the two sets of measurement values to diverge. One previous study comparing AS-OCT measurements from the Spectralis and Cirrus displayed a similar scaling effect as measurement values increased, although the authors did not comment on this finding.²⁰ We hypothesize that this systematic effect arises from how the different OCT devices account for corneal refraction, which is a parameter that is used to scale the corresponding OCT B-scans. Based on our findings, we recommend that anterior segment measurement values should not be used interchangeably between devices.

Anterior chamber width, or the distance between two scleral spurs, had lower intra- and inter-device ICC values for both devices compared to the other parameters. Intra-device variability in ACW measurements may arise from inter-scan differences in imaging location despite our best efforts to scan centered over the cornea with the CASIA and along the horizontal meridian with the Spectralis. As of now, neither device provides inter-scan image registration that ensures a fixed scan location. At first this appears problematic as all measurement values are dependent on the location of the scleral spur. Fortunately, measurements of the remaining parameters appear unaffected by the ACW variability, as indicated by high ICC values, low CoV values, and narrow limits of agreement. This reinforces the point that while significant anatomical variation occurs along the angle, localized changes are relatively small.¹⁴ However, the lack of inter-scan image registration could present a problem as our understanding of regional angle anatomy increases and a need to re-image specific portions of the angle emerges.

Our study has a few limitations. One is that we did not randomize the order of testing for the four scans. AS-OCT is a non-contact imaging modality and all scans were performed within a few minutes of each other. We did, however, control for factors that could independently affect the measurements, such as lighting conditions and pupil diameter. Additionally, the study sample size was relatively small. While there were only 38 intra-device and 40 inter-device comparisons for the angle parameters, the data showed strong correlations between measurements with narrow confidence intervals. Finally, we only used one trained observer to grade the images. Previous studies have demonstrated high intra-observer reproducibility of measurement values for other AS-OCT devices.^{15,16} Therefore, we decided this approach would be better than a multi-observer approach which would introduce additional variability to the measurements.^{21,24}

Our results demonstrate encouraging reproducibility of measurement values from the CASIA2 and Spectralis OCT2, an important quality if they are to be incorporated into clinical practice. Neither device appears to be superior to the other in this regard despite their different strengths and shortcomings. There are, however, systematic differences in measurements between the devices. Currently, there is no gold standard device to confirm the accuracy of AS-OCT devices and their image scaling algorithms. Until there is a reliable method to calibrate these devices, their data should not be used interchangeably across platforms for clinical and research purposes.

Acknowledgments

This work was supported by Vision Research Core Grant P30EY022589 from the National Eye Institute, National Institutes of Health, Bethesda, MD and by an unrestricted grant from Research to Prevent Blindness, Inc., New York, NY.

References

1. Seager FE, Jefferys JL, Quigley HA. Comparison of dynamic changes in anterior ocular structures examined with anterior segment optical coherence tomography in a cohort of various origins. *Invest Ophthalmol Vis Sci*. 2014; 55(3):1672–1683. [PubMed: 24557354]
2. Dastiridou AI, Pan X, Zhang Z, et al. Comparison of Physiologic versus Pharmacologic Mydriasis on Anterior Chamber Angle Measurements Using Spectral Domain Optical Coherence Tomography. *J Ophthalmol*. 2015; 2015:845643. [PubMed: 25878896]
3. Mak H, Xu G, Leung CK-S. Imaging the iris with swept-source optical coherence tomography: relationship between iris volume and primary angle closure. *Ophthalmology*. 2013; 120(12):2517–2524. [PubMed: 23850092]
4. Han S, Sung KR, Lee KS, Hong JW. Outcomes of laser peripheral iridotomy in angle closure subgroups according to anterior segment optical coherence tomography parameters. *Invest Ophthalmol Vis Sci*. 2014; 55(10):6795–6801. [PubMed: 25249604]
5. Jiang Y, Chang DS, Zhu H, et al. Longitudinal changes of angle configuration in primary angle-closure suspects: the Zhongshan Angle-Closure Prevention Trial. *Ophthalmology*. 2014; 121(9):1699–1705. [PubMed: 24835757]
6. Kronberg BP, Rhee DJ. Anterior segment imaging and the intraocular pressure lowering effect of cataract surgery for open and narrow angle glaucoma. *Semin Ophthalmol*. 27(5–6):149–154.
7. Shao T, Hong J, Xu J, Le Q, Wang J, Qian S. Anterior Chamber Angle Assessment by Anterior-segment Optical Coherence Tomography After Phacoemulsification With or Without Goniosynechialysis in Patients With Primary Angle Closure Glaucoma. *J Glaucoma*. 2015; 24(9):647–655. [PubMed: 24844542]
8. Hamanaka T, Omata T, Sekimoto S, Sugiyama T, Fujikoshi Y. Bleb analysis by using anterior segment optical coherence tomography in two different methods of trabeculectomy. *Invest Ophthalmol Vis Sci*. 2013; 54(10):6536–6541. [PubMed: 23989189]
9. Nongpiur ME, Aboobakar IF, Baskaran M, et al. Association of Baseline Anterior Segment Parameters With the Development of Incident Gonioscopic Angle Closure. *JAMA Ophthalmol*. 2017; 135(3):252. [PubMed: 28196218]
10. Leung CK-S, Weinreb RN. Anterior chamber angle imaging with optical coherence tomography. *Eye (Lond)*. 2011; 25(3):261–267. [PubMed: 21242985]
11. Cheung CY, Zheng C, Ho C-L, et al. Novel anterior-chamber angle measurements by high-definition optical coherence tomography using the Schwalbe line as the landmark. *Br J Ophthalmol*. 2011; 95(7):955–959. [PubMed: 21183513]
12. Kagemann L, Wollstein G, Ishikawa H, et al. Identification and assessment of Schlemm's canal by spectral-domain optical coherence tomography. *Invest Ophthalmol Vis Sci*. 2010; 51(8):4054–4059. [PubMed: 20237244]
13. Blieden LS, Chuang AZ, Baker LA, et al. Optimal number of angle images for calculating anterior angle volume and iris volume measurements. *Invest Ophthalmol Vis Sci*. 2015; 56(5):2842–2847. [PubMed: 25829412]
14. Xu BY, Israelsen P, Pan BX, Wang D, Jiang X, Varma R. Benefit of Measuring Anterior Segment Structures Using an Increased Number of Optical Coherence Tomography Images: The Chinese American Eye Study. *Invest Ophthalmol Vis Sci*. 2016; 57(14):6313–6319. [PubMed: 27893097]
15. Ho S-W, Baskaran M, Zheng C, et al. Swept source optical coherence tomography measurement of the iris-trabecular contact (ITC) index: a new parameter for angle closure. *Graefes Arch Clin Exp Ophthalmol*. 2013; 251(4):1205–1211. [PubMed: 23001586]
16. Aptel F, Chiquet C, Gimbert A, et al. Anterior Segment Biometry Using Spectral-Domain Optical Coherence Tomography. *J Refract Surg*. 2014; 30(5):354–360. [PubMed: 24694582]

17. Tun TA, Baskaran M, Zheng C, et al. Assessment of trabecular meshwork width using swept source optical coherence tomography. *Graefes Arch Clin Exp Ophthalmol*. 2013; 251(6):1587–1592. [PubMed: 23436037]
18. Leung CK, Cheung CYL, Li H, et al. Dynamic Analysis of Dark–Light Changes of the Anterior Chamber Angle with Anterior Segment OCT. *Investig Ophthalmology Vis Sci*. 2007; 48(9):4116.
19. Cicchetti DV. Guidelines, criteria, and rules of thumb for evaluating normed and standardized assessment instruments in psychology. *Psychol Assess*. 1994; 6(4):284–290.
20. Marion KM, Maram J, Pan X, et al. Reproducibility and Agreement Between 2 Spectral Domain Optical Coherence Tomography Devices for Anterior Chamber Angle Measurements. *J Glaucoma*. 2015; 24(9):642–646. [PubMed: 26200742]
21. Cumba RJ, Radhakrishnan S, Bell NP, et al. Reproducibility of Scleral Spur Identification and Angle Measurements Using Fourier Domain Anterior Segment Optical Coherence Tomography. *J Ophthalmol*. 2012; 2012:1–14.
22. Leung CK, Li H, Weinreb RN, et al. Anterior Chamber Angle Measurement with Anterior Segment Optical Coherence Tomography: A Comparison between Slit Lamp OCT and Visante OCT. *Investig Ophthalmology Vis Sci*. 2008; 49(8):3469.
23. Tan BB, Natividad M, Chua K-C, Yip LW. Comparison of Retinal Nerve Fiber Layer Measurement Between 2 Spectral Domain OCT Instruments. *J Glaucoma*. 2012; 21(4):266–273. [PubMed: 21637116]
24. Liu S, Yu M, Ye C, Lam DSC, Leung CK. Anterior Chamber Angle Imaging with Swept-Source Optical Coherence Tomography: An Investigation on Variability of Angle Measurement. *Investig Ophthalmology Vis Sci*. 2011; 52(12):8598.

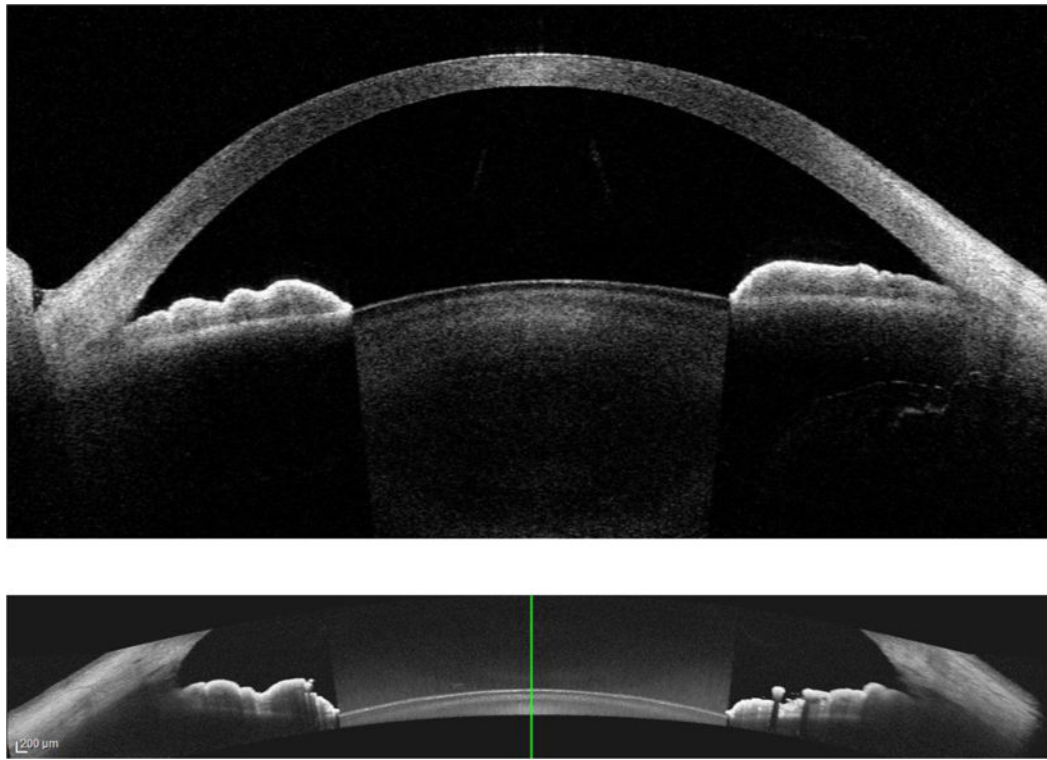


Figure 1.
Representative AS-OCT images from the CASIA2 (top) and Spectralis OCT2 (bottom).

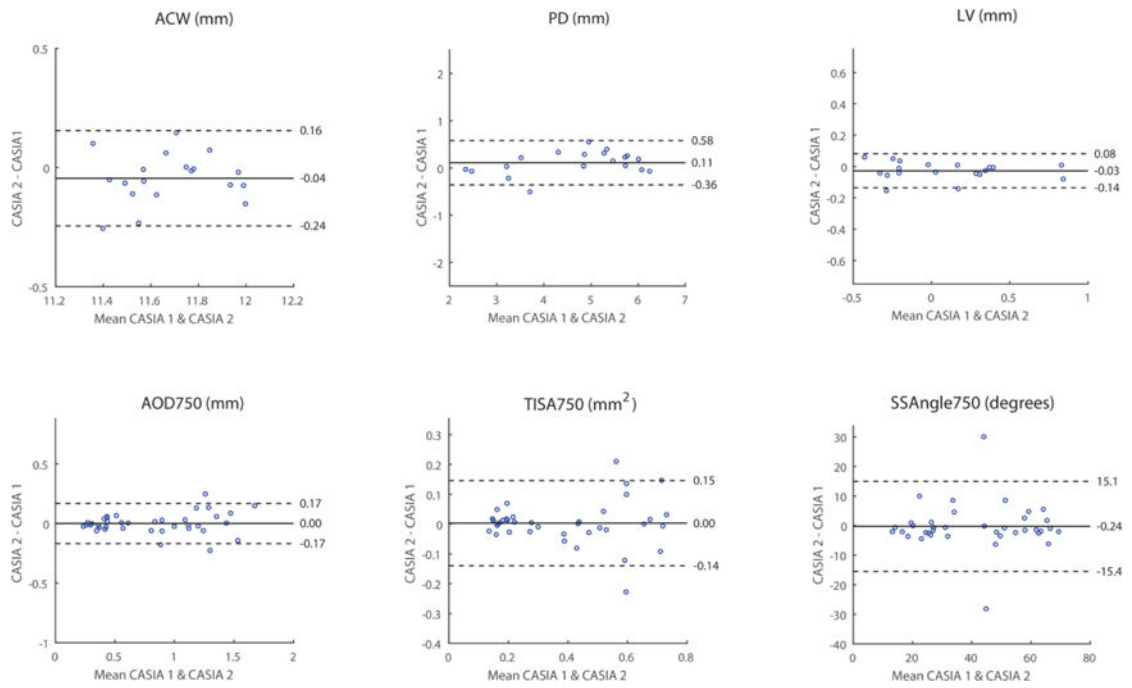


Figure 2. Intra-device reproducibility of CASIA measurement values. Bland-Altman plots for the two sets of measurement values (blue dots) are plotted for each parameter (heading). Each plot includes the mean difference (solid line) and limits of agreement (dotted lines; 95% confidence interval = 1.96 standard deviations).

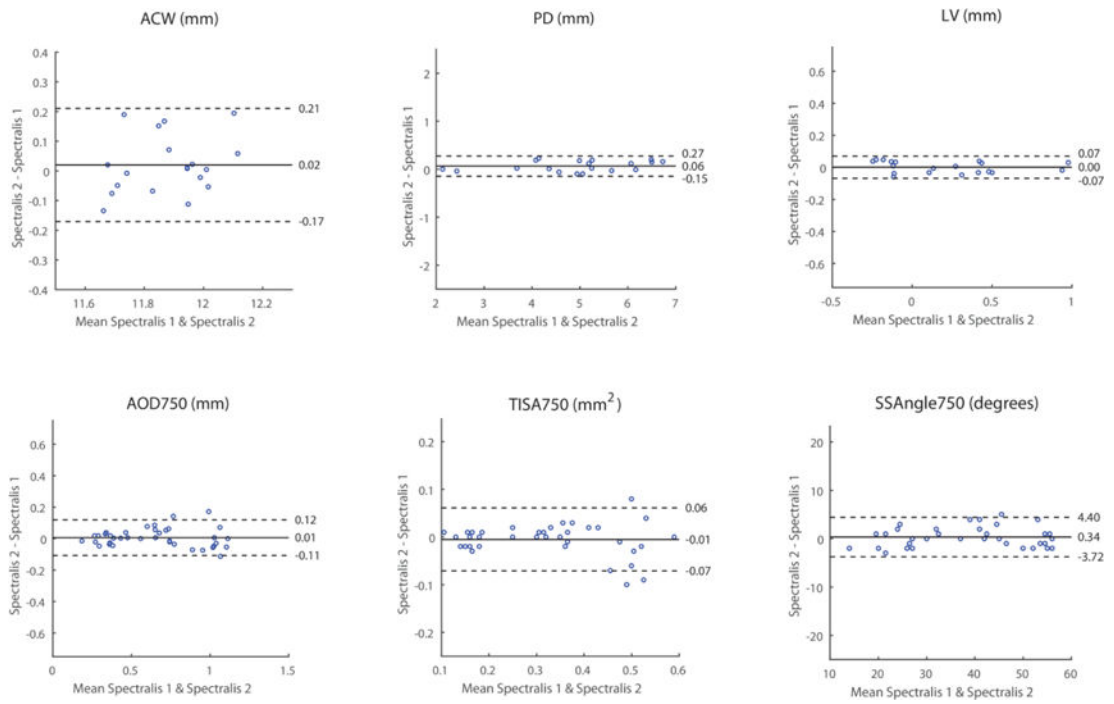


Figure 3. Intra-device reproducibility of Spectralis measurement values. Conventions are the same as Figure 2.

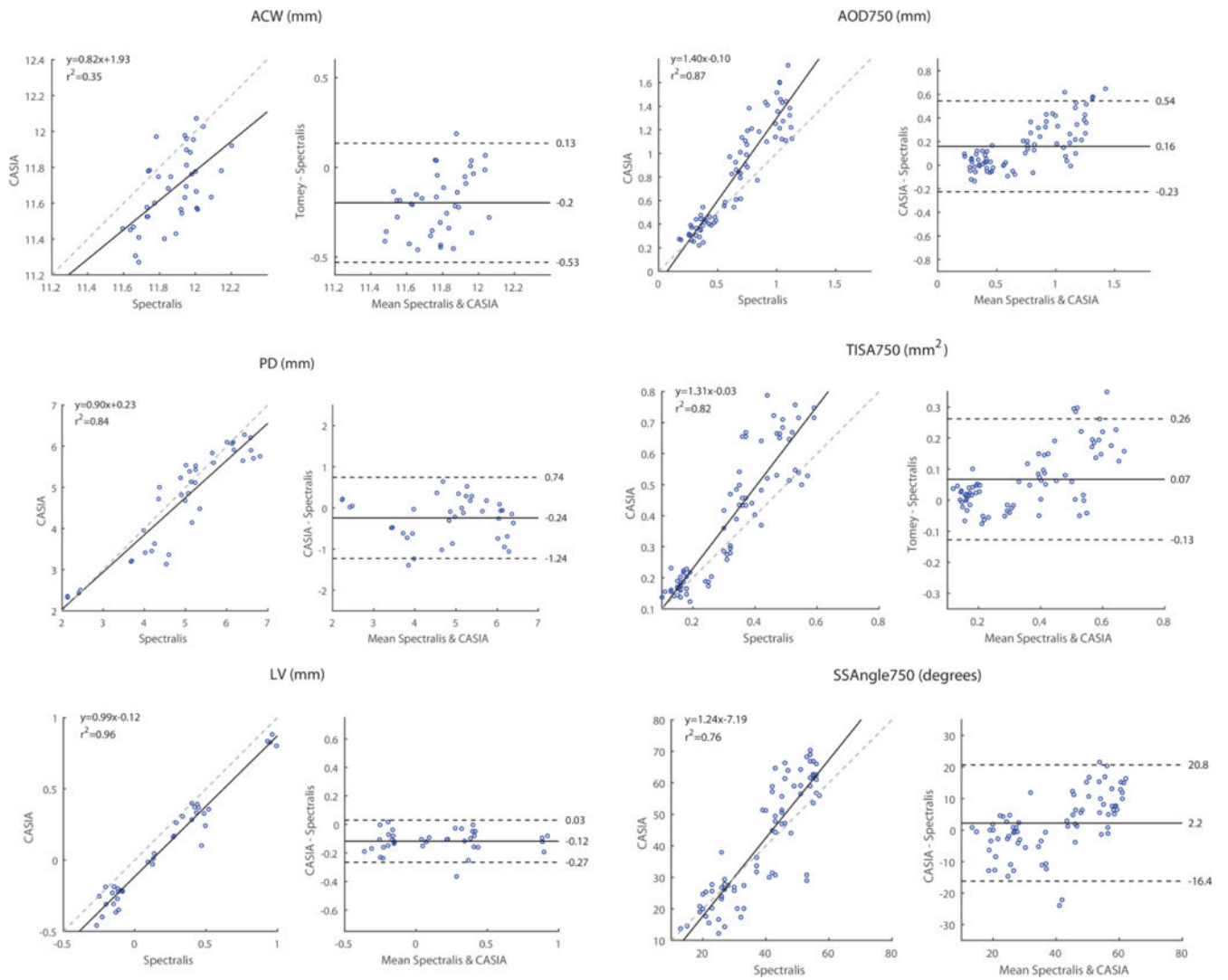


Figure 4. Inter-device reproducibility of CASIA and Spectralis measurement values. Conventions are the same as Figure 2. Linear regression plots (left) are shown in addition to Bland-Altman plots (right) plots. The linear regression model (solid line) and equivalence line (dotted line) are shown for each comparison.

Intra-device reproducibility of CASIA measurement values. Mean measurement values shown with standard deviations. Intra-class correlation coefficients (ICC), mean differences with limits of agreement (LoA), and coefficients of variation (CoV) also shown. PD, pupil diameter. LV, lens vault. ACW, anterior chamber width. AOD750, angle opening distance at 750um. TISA750, trabecular iris space area at 750um. SSAngle750, scleral spur angle at 750um.

Table 1

	CASIA 1	CASIA 2	ICC	95% CI	Mean diff	LoA	CoV (%)
PD (mm)	4.74 ± 1.28	4.63 ± 1.19	0.98	0.95 – 0.99	0.11	-0.36 – 0.58	5.09
LV (mm)	0.07 ± 0.37	0.09 ± 0.38	0.99	0.97 – 0.99	-0.03	-0.14 – 0.08	69.29
ACW (mm)	11.66 ± 0.21	11.70 ± 0.20	0.86	0.75 – 0.92	-0.04	-0.24 – 0.16	0.87
AOD750 (mm)	0.81 ± 0.45	0.81 ± 0.43	0.98	0.96 – 0.99	0.00	-0.17 – 0.17	10.60
TISA750 (mm2)	0.39 ± 0.21	0.39 ± 0.21	0.94	0.90 – 0.97	0.00	-0.14 – 0.15	14.79
SSAngle750 (degrees)	41.04 ± 18.36	41.28 ± 18.33	0.91	0.84 – 0.95	-0.24	-15.4 – 15.1	14.87

Table 2

Intra-device reproducibility of Spectralis measurement values.

	Spectralis 1	Spectralis 2	ICC	95% CI	Mean diff	95% CI	CoV (%)
PD (mm)	4.96 ± 1.27	4.90 ± 1.24	1.00	0.99 – 1.00	0.06	-0.15 – 0.27	2.18
LV (mm)	0.20 ± 0.37	0.20 ± 0.37	1.00	0.99 – 1.00	0.00	-0.07 – 0.07	17.89
ACW (mm)	11.89 ± 0.16	11.87 ± 0.14	0.79	0.63 – 0.88	0.02	-0.17 – 0.21	0.82
AOD750 (mm)	0.65 ± 0.29	0.65 ± 0.29	0.98	0.96 – 0.99	0.01	-0.11 – 0.12	8.88
TISA750 (mm²)	0.32 ± 0.14	0.32 ± 0.15	0.97	0.95 – 0.99	-0.01	-0.07 – 0.06	10.51
SSAngle750 (degrees)	39.11 ± 12.99	38.76 ± 12.80	0.99	0.98 – 0.99	0.34	-3.72 – 4.06	5.35

Table 3

Inter-device reproducibility of CASIA and Spectralis measurement values.

	CASIA	Spectralis	ICC	95% CI	Mean diff	LoA
PD (mm)	4.69 ± 1.23	4.93 ± 1.25	0.90	0.85 – 0.94	-0.24	-1.24 – 0.74
LV (mm)	0.08 ± 0.37	0.20 ± 0.37	0.93	0.89 – 0.96	-0.12	-0.27 – 0.03
ACW (mm)	11.68 ± 0.21	11.88 ± 0.15	0.20	-0.02 – 0.41	-0.20	-0.53 – 0.13
AOD750 (mm)	0.81 ± 0.44	0.65 ± 0.29	0.78	0.67 – 0.85	0.16	-0.23 – 0.54
TISA750 (mm ²)	0.39 ± 0.21	0.32 ± 0.14	0.78	0.68 – 0.85	0.07	-0.13 – 0.26
SSAngle750 (degrees)	41.16 ± 18.22	38.93 ± 12.81	0.81	0.72 – 0.88	2.20	-16.4 – 20.8